AEM
Journals.ASM.org

Identification of Benzo[*a*]pyrene-Metabolizing Bacteria in Forest Soils by Using DNA-Based Stable-Isotope Probing

Mengke Song,[a] Chunling Luo,[a] Longfei Jiang,[a] Dayi Zhang,[b] Yujie Wang,[c] Gan Zhang[a]

Guangzhou Institute of Geochemistry, Chinese Academy of Sciences, Guangzhou, China[a]; Lancaster Environment Centre, Lancaster University, Lancaster, United Kingdom[b]; School of Environmental Science and Engineering, Guangdong University of Technology, Guangzhou, China[c]

DNA-based stable-isotope probing (DNA-SIP) was used in this study to investigate the uncultivated bacteria with benzo[*a*]pyrene (BaP) metabolism capacities in two Chinese forest soils (Mt. Maoer in Heilongjiang Province and Mt. Baicaowa in Hubei Province). We characterized three different phylotypes with responsibility for BaP degradation, none of which were previously reported as BaP-degrading microorganisms by SIP. In Mt. Maoer soil microcosms, the putative BaP degraders were classified as belonging to the genus *Terrimonas* (family *Chitinophagaceae*, order *Sphingobacteriales*), whereas *Burkholderia* spp. were the key BaP degraders in Mt. Baicaowa soils. The addition of metabolic salicylate significantly increased BaP degradation efficiency in Mt. Maoer soils, and the BaP-metabolizing bacteria shifted to the microorganisms in the family *Oxalobacteraceae* (genus unclassified). Meanwhile, salicylate addition did not change either BaP degradation or putative BaP degraders in Mt. Baicaowa. Polycyclic aromatic hydrocarbon ring-hydroxylating dioxygenase (PAH-RHD) genes were amplified, sequenced, and quantified in the DNA-SIP ^{13}C heavy fraction to further confirm the BaP metabolism. By illuminating the microbial diversity and salicylate additive effects on BaP degradation across different soils, the results increased our understanding of BaP natural attenuation and provided a possible approach to enhance the bioremediation of BaP-contaminated soils.

Polycyclic aromatic hydrocarbons (PAHs), a class of persistent organic pollutants (POPs), enter the environment through both natural and anthropogenic pathways. PAHs are released into the environment by means of natural processes, such as forest fires and direct biosynthesis under the action of microbes and plants (1). The primary artificial source of PAHs is the incomplete combustion of organic matter at high temperatures caused by human activities (2). Their presence in the environment poses a severe threat to public and ecosystem health because of their known acute toxicity and mutagenic, teratogenic, and carcinogenic features; they are therefore classified as priority pollutants by the U.S. Environmental Protection Agency (3). Furthermore, the persistence and genotoxicity of PAHs increase with molecular weight, and the presence of high-molecular-weight (HMW) PAHs in the environment is of greater concern. Benzo[*a*]pyrene (BaP), a representative HMW PAH with a five-ring structure, is a widespread pollutant with potent mutagenic and carcinogenic properties (4, 5). BaP is therefore identified as the first class of "human carcinogens" according to the report of the World Health Organization (WHO) International Agency for Research on Cancer (6). Generally, in soils with no industrial contamination, BaP concentrations vary from 3.5 to 3,700 μg/kg, with a median concentration of 16 μg/kg of soil; in contaminated soils and sediments, BaP concentrations range from 82 to 536 mg/kg (7).

Bacteria possessing the ability of BaP utilization are readily isolated from contaminated soils or sediments, and most of our current knowledge about BaP metabolism by microbes has been gained from such isolates (8–10). The functional PAH-RHD genes (encoding PAH-ring hydroxylating dioxygenase enzymes) have also been examined to understand BaP degradation mechanisms, such as *nah*, *pah*, *arh*, and *phn* genes in Gram-negative (GN) bacteria and the evolutionarily correlated *nid*, *nir*, *phd*, and *nar* genes in Gram-positive (GP) bacteria, which are responsible for the first step of PAHs (naphthalene, phenanthrene, anthracene, and pyrene) hydroxylation under aerobic conditions (11, 12). Terminal dioxygenase is the component of PAH-RHD, composed of large α- and small β-subunits. The genes coding for the mononuclear iron-containing catalytic domain (a conserved region) of PAH-RHDα (α-subunit) have been widely used for studying RHD diversity and the PAH degradation potential by bacteria in the environment (11). In addition to the research on the genes involved in PAH degradation, studies using culture-dependent tools to investigate the degrading capacity of BaP degraders showed that rare bacteria were capable of metabolizing BaP without metabolic intermediate additives (9, 10, 13); in most cases, BaP degradation is stimulated by the addition of some intermediates produced during BaP metabolism (14, 15). These intermediates possess the ability of stimulating PAH dioxygenase activity and are capable of supplying electrons for NAD (NADH) coenzymes, which are necessary for the functions of oxygenase enzymes, to initiate aerobic PAH degradation (8, 16). Salicylate is a classic intermediate, inducing PAHs metabolism of PAHs-degrading bacteria and selectively stimulating their growth (8, 16, 17). The addition of salicylate to contaminated soils or sediments has been proposed as a means of encouraging PAH degradation during bioremediation

Received 14 June 2015 **Accepted** 2 August 2015

Accepted manuscript posted online 7 August 2015

Citation Song M, Luo C, Jiang L, Zhang D, Wang Y, Zhang G. 2015. Identification of benzo[*a*]pyrene-metabolizing bacteria in forest soils by using DNA-based stable-isotope probing. Appl Environ Microbiol 81:7368–7376. doi:10.1128/AEM.01983-15.

Editor: H. Nojiri

Address correspondence to Chunling Luo, clluo@gig.ac.cn.

Supplemental material for this article may be found at http://dx.doi.org/10.1128/AEM.01983-15.

This article is contribution no. IS-2125 from GIGCAS.

(16). *Sphingomonas yanoikuyae* JAR02 was reported to completely remove BaP (1.2 mg/liter) within 20 h in the aqueous phase with additive salicylate (8). Additionally, *Pseudomonas saccharophila* P15 isolated from creosote-contaminated soil improved BaP removal after the addition of salicylate, which acted as the inducer of PAH dioxygenase activity (16).

The traditional culture-dependent approaches, such as isolating and cultivating target bacteria in the laboratory, suffer from the fact that <1% of the soil microorganisms are cultivable. The process underestimates the diversity of the prokaryotes and fails to capture the true nature of the complex interactions within microbial communities at a specific site. The uncultured bacteria may possess an unexplored reservoir of novel and valuable gene-encoding catalysts that benefit bioremediation, industry, and medicine (18–20). Furthermore, with our limited understanding of the actual biota, cultivation presents challenges for field bioremediation (21). In recent years, stable-isotope probing (SIP) has emerged as a culture-independent method to identify microorganisms capable of utilizing specific substrates in complex environments. Microbial populations responsible for the degradation of targeted contaminants are labeled by stable isotopes and then characterized (22–25). To date, many bacteria have been successfully identified by SIP with their unique capabilities of metabolizing phenolic compounds and PAHs, such as naphthalene (25, 26), anthracene (27), phenanthrene (26), pyrene (23, 28), fluoranthene (29), benz[a]anthracene (29), biphenyl (30, 31), phenol (31), and benzoate (31). However, to our knowledge, no study until now has examined BaP-degrading bacteria successfully using SIP.

In the present study, to investigate the microorganisms responsible for BaP degradation in the uncontaminated soil, [^{13}C]DNA-targeted SIP was applied to two Chinese forest soils from Mt. Maoer and Mt. Baicaowa. The influence of salicylate on BaP biodegradation was further studied, as was its role in functional microbial community dynamics. By sequencing and quantifying (by real-time quantitative PCR [qPCR]) PAH-RHDα genes in [^{13}C]DNA enriched fraction, our work further revealed the BaP metabolism in uncontaminated soil and the stimulating effects of salicylate addition varying among different soils. To our knowledge, this study successfully applied the culture-independent SIP technique to characterize BaP-degrading bacteria in forest soil and provided an important contribution to the understanding of BaP biodegradation in complex communities and the bioremediation of HMW PAH-contaminated soil.

MATERIALS AND METHODS

Soil samples. Soil samples were collected from Mt. Maoer (45°22′48″N, 127°40′48″E) in Heilongjiang Province, and Mt. Baicaowa (40°48′36″N, 117°35′60″E) in Hebei Province, China. The pH and total organic carbon content were 7.5 and 16.0% (Mt. Maoer) and 6.0 and 12.3% (Mt. Baicaowa), respectively. Before use, large objects in the soils, such as stones and debris, were removed manually in the laboratory. The soil samples were then homogenized, sieved through a 2-mm-pore-size screen, and prepared for the BaP degradation treatment.

Setup of BaP-degrading microcosms. Both non-salicylate- and salicylate-additive treatments were included for the two forest soils. Here, BS and B represent the Mt. Baicaowa soils amended with and without salicylate, and MS and M denote the Mt. Maoer soils amended with and without salicylate, respectively. The experiments were conducted as follows. Three grams of soil (dry weight) was placed in a 150-ml serum bottle containing 10 ml of phosphate-buffered mineral medium (32). The bottles were sealed with rubber stoppers and compressed with an aluminum seal. The unlabeled BaP (99%) or [^{13}C]BaP ([$^{13}C_4$]BaP; 99%; Fig. S1 in the supplemental material shows the position of ^{13}C-labeled carbons), both from Cambridge Isotope Laboratories, Inc., and dissolved in nonane with a final concentration of 100 mg/liter, was added to the respective bottles using a gastight syringe to give a final BaP concentration of 1 mg/kg. For salicylate-additive treatments, the final salicylate concentration was 10 mg/kg. Two negative-control treatments were included as no-carbon-source (CK) and nonbioactive (sterilized by gamma irradiation; ^{12}C-NB). Two positive treatments were amended with [^{12}C]BaP and [^{13}C]BaP carbon sources, named as ^{12}C-BT and ^{13}C-BT, respectively. Eight samples were prepared for each treatment. The microcosms were incubated at room temperature (~25°C) with reciprocal shaking at a speed of 120 rpm/min. On days 7, 14, 28, and 42 after incubation, two samples from each treatment were sacrificed for BaP analysis and DNA extraction, respectively. All stock solutions were filtered through 0.2-μm-pore-size filters and stored in dark brown containers. To prepare sterile controls, soils were gamma irradiated (50 kGy) for 2 h before use.

BaP analysis. The ^{12}C-NB, ^{12}C-BT, and ^{13}C-BT samples were prepared for BaP analysis using the following steps. The serum bottles were frozen at −20°C overnight, followed by freeze-drying using a vacuum freeze dryer. The dry soil samples were then homogenized, pulverized, spiked with 1,000 ng of deuterated PAHs as surrogate standards, and extracted with dichloromethane (DCM) in a Soxhlet apparatus for 48 h, with the addition of activated copper to remove sulfur. The extract was concentrated to ~0.5 ml after solvent exchange to hexane. The soil extracts were purified in a multilayer silica gel-alumina column (8-mm internal diameter) filled with anhydrous Na_2SO_4 (1 cm), neutral silica gel (3 cm, 3% [wt/wt]; deactivated), and neutral alumina (3 cm, 3% [wt/wt]; deactivated; from top to bottom) via elution with 15 ml of hexane-DCM (1:1 [vol/vol]). After concentrating to ~50 μl under a gentle stream of N_2, 1,000 ng of hexamethylbenzene was added as an internal standard prior to analysis.

BaP was detected on an Agilent 7890 gas chromatograph equipped with a capillary column (DB-5MS, 30 m, 0.25 mm, 0.25 μm) and a mass spectrometric detector (MSD; Agilent 5975). One microliter of sample was injected in splitless mode with a 10-min solvent delay time. High-purity helium was used as the carrier gas at a flow rate of 1.83 ml/min. The temperatures of the injector and transfer lines were 290 and 300°C, respectively. The initial oven temperature was set at 60°C for 1 min, rising to 290°C at a rate of 3°C/min, and was subsequently held constant for 20 min. PAH standards were used to quantify BaP. Instrumental performance was subjected to quality control calibration with the standards after each set of eight samples had been analyzed. Six PAH standard concentrations were used to derive the calibration curves. Concentrations were corrected using reference to surrogate recovery levels.

DNA extraction and ultracentrifugation. Samples from ^{12}C-BT and ^{13}C-BT were both prepared for biotic analysis at 7, 14, 28, and 42 days of cultivation. The total genomic DNA was extracted from 1.0-g quantities of soils with triplicates using the Powersoil DNA isolation kit (MO BIO Laboratories, Inc.) according to the manufacturer's protocol. DNA concentrations were determined using an ND-2000 UV-visible (UV-Vis) spectrophotometer (NanoDrop Technologies). Subsequently, ~10,000 ng of DNA was added to Quick-Seal polyallomer tubes (13 by 51 mm, 5.1 ml; Beckman Coulter), along with a Tris-EDTA (TE; pH 8.0)-cesium chloride (CsCl) solution. Before the tubes were sealed with cordless quick-seal tube topper (Beckman Coulter), the average buoyant density (BD) of all prepared gradients was determined with an AR200 digital refractometer (Leica Microsystems Inc.) and adjusted to ~1.77 g/ml by adding a CsCl solution or Tris-EDTA buffer, if necessary. The tubes were transferred to an ultracentrifuge (Optima L-100XP; Beckman Coulter) and centrifuged at 178,000 × *g* (20°C) for 48 h. Following centrifugation, 150-μl fractions were collected from each tube using a fraction recovery system (Beckman Coulter). The BD of each fraction was measured, and the CsCl was further removed by glycogen-assisted ethanol precipitation (33).

PCR and TRFLP. The fractions were subjected to terminal restriction fragment length polymorphism (TRFLP) analysis using standard procedures (24). Briefly, DNA was amplified with 27F-FAM (5′-AGAGTTTG ATCMTGGCTCAG; 5′ end labeled with carboxyfluorescein) and 1492R (5′-GGTTACCTTGTTACGACTT) using the following PCR program: initial melting at 94°C for 5 min, 30 amplification cycles at 94°C for 30 s, 55°C for 30 s, and 72°C for 1.5 min, and a final extension at 72°C for 10 min. After amplification, the presence of PCR products was confirmed by 1% agarose gel electrophoresis. The PCR products were purified using an EZNA Cycle-Pure kit (Omega Bio-Tek, Inc.) by following the manufacturer's instructions and digested with HaeIII (New England BioLabs) for 4 to 5 h at 37°C. One nanogram of each labeled PCR product was analyzed on an ABI 3730 genetic analyzer (Applied Biosystems) running Peak Scanner software version 1.0 (Applied Biosystems). A GeneScan ROX 500 set of internal standards (Applied Biosystems) was used. The percent abundance of each fragment was determined as previously described (30).

Identification of the PAH-RHD$_\alpha$ gene in microcosms and enumeration in SIP fractions. As the PAH-RHD$_\alpha$ genes possessed by GN and GP bacteria do not belong to a monophyletic cluster (12), the presence of the PAH-RHD$_\alpha$ genes was investigated using PAH-RHD$_\alpha$ GP primers (641F, 5′-CGGCGCCGACAAYTTYGTNGG, and 933R, 5′-GGGGAACACGGT GCCRTGDATRAA) and PAH-RHDα GN primers (610F, 5′-GAGATGC ATACCACGTKGGTTGGA, and 911R, 5′-AGCTGTTGTTCGGGAA GAYWGTGCMGTT) (32) on the heavy DNA fractions from B, BS, M, and MS microcosms. A gradient PCR was performed with annealing temperatures ranging from 52 to 62°C. Amplification reactions were carried out in a volume of 50 μl, as previously described (12).

The copy number of the PAH-RHDα sequences in fractions from ^{13}C-labeled and unlabeled DNA was determined by qPCR using the PAH-RHDα GP primers, because only one strong and specific amplicon amplified with PAH-RHDα GP primers was produced from the heavy fractions in M and MS microcosms in this work. The PCR mixture contained 10 μl of SYBR green PCR Premix *Ex Taq* II (TaKaRa Bio) and 1 μl of DNA template in a final volume of 20 μl. A standard curve was obtained by producing 10 dilution series of plasmid pGEM-T Easy vector sequences (10^2 to 10^8 copies; Promega) containing the PAH-RHDα gene detected in M and MS treatments with the PAH-RHDα GP primers (641F, 5′-CGG CGCCGACAAYTTYGTNGG, and 933R, 5′-GGGGAACACGGTGCCRT GDATRAA). The amplification reactions were conducted using a two-step method in a 48-well optical plate on an Eco real-time PCR system (Illumina) as follows: denaturation for 10 min at 95°C, followed by 40 cycles of 10 s at 95°C and 30 s at 60°C; then the SYBR green signal intensities were measured after the 30-s step at 60°C. At the end of the real-time PCR, a melting-curve analysis was performed by increasing the temperature from 55 to 95°C. For each DNA sample, the average of three replicates was determined as the copy number per fraction.

Sequencing of partial PAH-RHDα and 16S rRNA genes. The 16S rRNA genes from the heavy fractions ([^{13}C]DNA, marked with a star in Fig. 1) corresponding to the peak in all panels of Fig. 1 with the BD values of 1.7198 g/ml, 1.7203 g/ml, 1.7165 g/ml, and 1.7100 g/ml, as well as the amplicons generated with the PAH-RHDα GP primer pair in M and MS treatments, were cloned and sequenced. Briefly, the 16S rRNA gene was amplified using a similar process to that described above, except the 27F-FAM primer was replaced by 27F. The purified PCR products were cloned into a pGEM-T Easy vector and transformed into *Escherichia coli* JM 109 (TaKaRa Bio). *E. coli* clones were then grown on Luria-Bertani medium solidified with 15 g/liter of agar in the presence of 50 μg/liter of ampicillin for 16 h at 37°C, and, finally, 100 clones with inserts were selected to be sequenced. The plasmids with target genes were extracted using an EZNA plasmid minikit (Omega Bio-Tek, Inc.), and the recombinants were selected using 0.8% agarose gel electrophoresis and sequenced on an ABI 3730 genetic analyzer using M13 primers. Sequence similarity searches and alignments were performed using the Basic Local Alignment Search Tool (BLAST) algorithm (National Center for Biotechnology Information) and Molecular Evolutionary Genetics Analysis (MEGA 5.1).

Nucleotide sequence accession numbers. The obtained 16S rRNA gene and the partial RHD gene sequences are available in GenBank (accession numbers KM267480 to KM267482 for partial 16S rRNA gene sequences of a 196-bp terminal restriction fragment [TRF] in B and BS treatments, 450-bp TRF in M treatment, and 216-bp TRF in MS treatment; KM267486 was used for the partial PAH-RHDα gene sequence).

RESULTS

BaP biodegradation in soils. BaP biodegradation in the four treatments (B, BS, M and MS) is briefly listed in Table 1. The recovery rates of BaP during the extraction procedure were 80% to 90% in this work (see Table S2 in the supplemental material). The BaP concentration in sterile treatments showed less decline than in unsterilized treatments. For instance, the residual BaP were 80.6%, 72.6%, 81.0%, and 69.7% for the ^{12}C-NB of B, BS, M and MS microcosms, respectively. Significant BaP biodegradation was observed in the unsterilized microcosms. For B and BS treatments (Table 1), BaP degradation achieved 16.6% and 18.1%, respectively, after 7 days of cultivation, and 33.4% and 31.1% of BaP was removed after 28 days. No significant BaP degradation difference was found between the B and BS treatments throughout the whole process, indicating the limited impact of salicylate on the capacities of BaP-degrading bacteria. The BaP degradation in M and MS treatments was much faster than those from Mt. Baicaowa. For example, 32.1% and 47.4% of BaP was removed in M and MS samples after 14 days of cultivation, compared to the corresponding degradation efficiency of 24.9% and 23.0% in B and BS samples. Salicylate significantly accelerated BaP biodegradation in soils from Mt. Maoer, where BaP removal efficiency was 32.1%, 43.7%, and 45.7% in M treatments at 14, 28, and 42 days, compared to the corresponding 47.4%, 52.5%, and 55.8% in MS treatments (Table 1).

Microbial structure analysis via SIP and TRFLP. DNA extracts from ^{12}C-BT and ^{13}C-BT soil samples were subjected to ultracentrifugation and fractionation, followed by TRFLP for each fraction. The organisms responsible for ^{13}C assimilation were detected by the relative abundances of specific TRFs between the control (^{12}C-BT) and the treatment with ^{13}C-labeled BaP (^{13}C-BT) at all three sampling points for each fraction.

In B microcosms, the TRFLP results (Fig. 1) indicated that the 196-bp HaeIII TRF at higher buoyant densities (1.7176 to 1.7328 g/ml) was enriched at 7, 14, and 28 days (16.6%, 24.9%, and 33.4% BaP removal, respectively) in ^{13}C-BT samples and that its relative abundance increased with time. Such enrichment and increasing trend were not observed in the ^{12}C-BT controls. Additionally, the enrichment of the 196-bp HaeIII TRF in the heavy fractions was also supported by their higher fluorescence intensity in the 28-day treatments (see Fig. S2A in the supplemental material), suggesting that ^{13}C was incorporated by the microorganisms represented by the 196-bp HaeIII TRF. To identify the BaP-degrading bacteria and obtain the phylogenetic affiliation of the 196-bp HaeIII TRF, the 16S rRNA clone library derived from the ^{13}C heavy fractions was sequenced, and the clones with the 193-bp HaeIII TRF cut site matched the TRFLP results for the 196-bp TRFs. The slight difference (2 or 3 bases) between the measured fragment lengths and those predicted using sequence data has been noted in previous studies (24, 34, 35). Based on the comparative analyses of 16S rRNA, the bacteria represented by the 196-bp TRF were classified as members of the genus *Burkholderia* (see Fig. S3). Additionally, a partial sequence with the predicted 213-bp HaeIII cut site in the

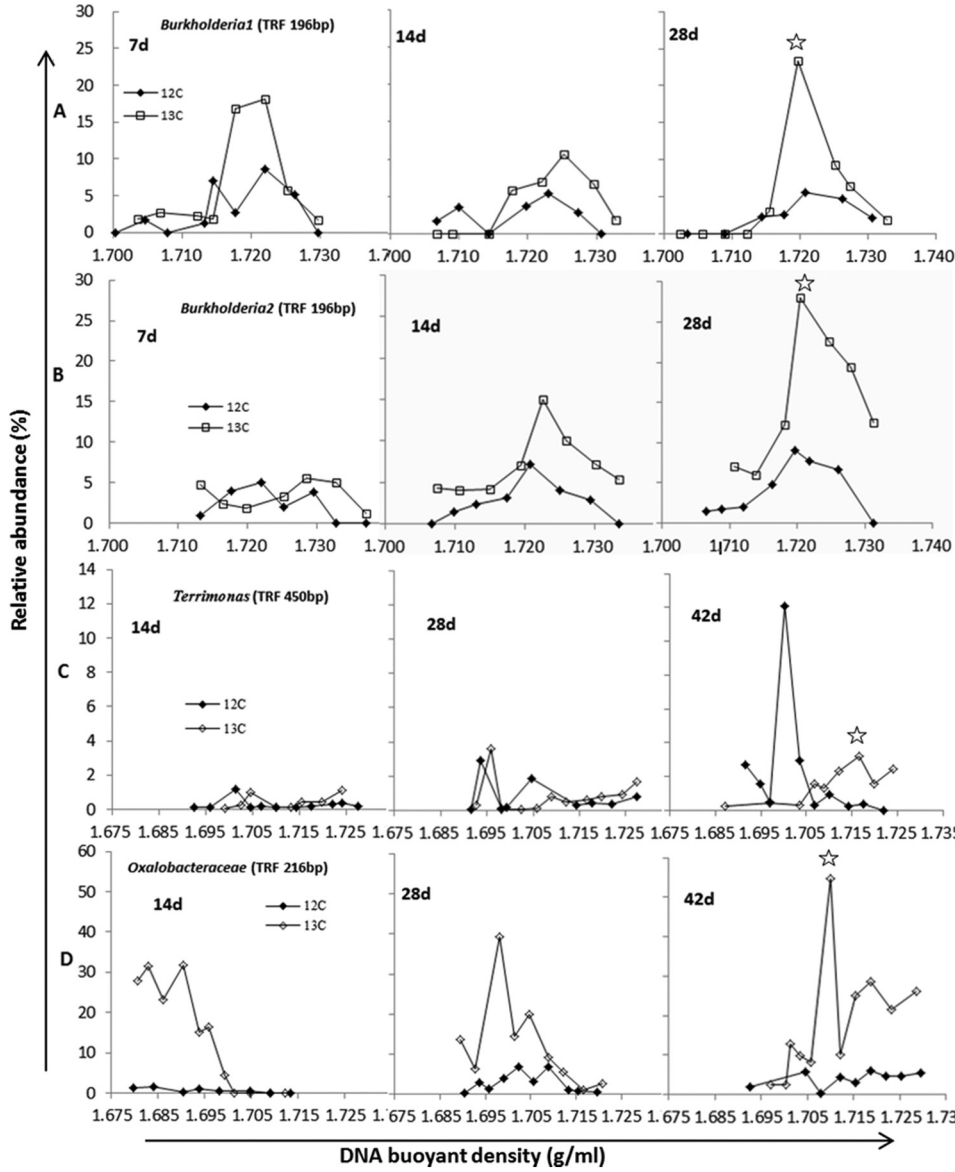

FIG 1 Relative abundances of TRFLP fragments (digested by HaeIII) assigned to *Burkholderia* 1 (from the treatment constructed with the Mt. Baicaowa soil [treatment B]) (A), *Burkholderia* 2 (from the treatment constructed with salicylate and soil of Mt. Baicaowa [treatment BS]) (B), *Terrimonas* (C), and *Oxalobacteraceae* (D) against the buoyant density gradients in B, BS, M, and MS treatments.

clone library was related to the class *Acidobacteria*. An additional member with the predicted 206-bp HaeIII cut site in the clone library was related to the genus *Rhodanobacter* (see Table S1).

In BS microcosms with salicylate addition, the bacteria represented by the 196-bp HaeIII TRF were involved in BaP biodegradation, as shown by DNA-SIP. Figure 1A illustrates a clear increasing relative abundance of 196-bp HaeIII TRF at higher BD (>1.7203 g/ml) in the ^{13}C-BT samples than in the ^{12}C-BT samples

TABLE 1 Percentage of BaP remaining in soils over time[a]

Time (days)	B (%)			BS (%)			M (%)			MS (%)		
	^{12}C-NB	^{12}C-BT	^{13}C-BT	^{12}C-NB	^{12}C-BT	^{13}C-BT	^{12}C-NB	^{12}C-BT	^{13}C-BT	^{12}C-NB	^{12}C-BT	^{13}C-BT
7	87.1	70.5	71.3	85.3	67.2	66.3	—	—	—	—	—	—
14	78.4	53.5	52.7	83.1	60.1	62.1	88.9	56.8	59.7	72.9	25.6	24.8
28	80.6	47.2	48.6	72.6	41.5	41.5	82.0	38.3	37.9	70.4	17.9	18.2
42	—	—	—	—	—	—	81.0	35.4	36.4	69.7	13.9	11.7

[a] ^{12}C-NB represents the nonbioactive sterile treatment, ^{12}C-BT represents the treatment with [^{12}C]BaP as the sole carbon sources, and ^{13}C-BT represents the treatment with [^{13}C]BaP as the sole carbon sources. B and BS represent the soil microcosms from Mt. Baicaowa amended without/with salicylate, whereas M and MS refer to the soil microcosms from Mt. Maoer amended without/with salicylate. —, samples were not set at the time.

at 7, 14, and 28 days. Furthermore, in the ^{13}C-BT samples after 28 days of cultivation, the BD value of the strongest fluorescence intensity of the 196-bp HaeIII TRF was higher than that of the ^{12}C-BT samples (see Fig. S2B). When the 16S rRNA clone library derived from the ^{13}C heavy fractions was inspected (see Table S1), 43 of the 100 clones with the predicted 193-bp HaeIII cut site fell in the order *Burkholderiales*. These clones were associated with BaP degradation, the same as the BaP degraders in B treatment. Additionally, three different clones with the predicted 362-, 217-, and 202-bp HaeIII cut sites were classified within the order *Burkholderiales*, and one clone with the predicted 212-bp HaeIII cut site shared 100% similarity with *Acidobacteria* strain Gp3, which also occurred in the heavy fraction of B treatment.

In M microcosms, the TRFLP fraction profiles (Fig. 1C) and the fluorescence intensity at 42 days (see Fig. S2C in the supplemental material) indicated relatively more abundant 450-bp HaeIII TRF in the heavy fractions (BD >1.7121 g/ml) of ^{13}C-BT samples but not in ^{12}C-BT samples. Furthermore, the relative abundance of the 450-bp HaeIII TRF in the heavy fraction increased with time in ^{13}C-BT samples, and the magnitude of the increase was largest for the sample that had been left the longest. For the ^{12}C-BT samples, the increase occurred in the light fraction (BD < 1.7045 g/ml), indicating ^{13}C-BaP assimilation by the bacteria represented by the 450-bp HaeIII TRF. However, this was not the dominant TRFLP fragment in the heavy fractions from ^{13}C-BT samples, and the other three TRFs (237, 372, and 215 bp) were the major members. Nevertheless, those microorganisms were not responsible for ^{13}C-BaP degradation, since a similar abundance was found in the heavy fractions of the ^{12}C-BT samples. The sequence of 16S rRNA clone libraries with the predicted 447-bp cut site fitted well with the TRFLP results. They were assigned to the genus *Terrimonas* (phylum *Bacteroidetes*, class *Sphingobacteria*, order *Sphingobacteriales*, family *Chitinophagaceae*), belonging most closely to the *Flavisolibacter ginsengiterrae* strain Gsoil 492 (see Fig. S4). Three clones with predicted 237-, 372-, and 215-bp HaeIII cut sites also appeared in the 16S rRNA clone library derived from the ^{13}C heavy fractions (see Table S1), and they were classified in the genus *Spartobacteria incertae sedis*, class *Acidobacteriaceae*, and family *Oxalobacteraceae*, respectively.

In MS treatment with salicylate addition, the 216-bp HaeIII TRF was involved in the BaP biodegradation and was enriched as the dominant TRF in the heavy fractions (BD > 1.7056 g/ml) at 28 and 42 days (Fig. 1D; see also Fig. S2D in the supplemental material). An increasing relative abundance was also observed for 14 to 42 days of cultivation in treatments amended with [^{13}C]BaP but not in ^{12}C-BT samples (Fig. 1D). Such an increase suggested that microorganisms represented by the 216-bp TRF were responsible for ^{13}C substrate uptake ([^{13}C]BaP degradation). Additionally, the relative abundances and fluorescence intensities of the 77-, 200-, and 450-bp TRFs (see Fig. S2D) were also high in the heavy fractions but lower than the 216-bp TRF in the ^{13}C-BT samples. The BD values of the three TRFs and their trends of relative abundance were similar between ^{13}C-BT and ^{12}C-BT treatments at the three sampling times. Hence, the microorganisms represented by the three TRFs were not directly involved in BaP degradation, and the large proportion of TRFs in the fractions might be due to their tolerance to BaP. Clones with the 216-bp HaeIII cut site from 16S rRNA clone libraries matched the TRFLP results, classified as members of the family *Oxalobacteraceae* (phylum *Proteobacteria*, class *Betaproteobacteria*, order *Burkholderiales*), also present in MS

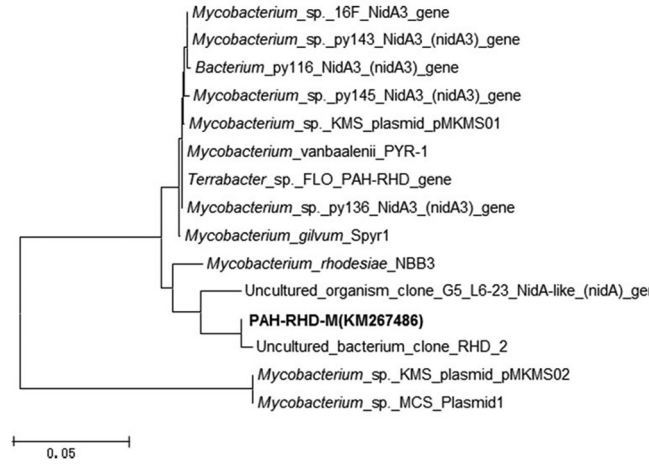

FIG 2 Phylogenetic tree of PAH-RHDα-M genes from MS (microcosms from Mt. Maoer soil amended with salicylate) and M (microcosms from Mt. Maoer soil without salicylate) treatments along with the closest matches in GenBank, constructed with MEGA 5.0 software using the neighbor-joining method.

[^{13}C]BaP treatment and sharing 98% sequence similarity with *Janthinobacterium lividum* strain DSM 1522 (see Fig. S5). Clones with 77-, 200-, and 447-bp HaeIII cut sites were classified in the order *Actinomycetales*, family *Burkholderiaceae*, and genus *Terrimonas*, respectively (see Table S1, MS).

Occurrence and quantification of PAH-RHDα genes in the SIP fractions. In B, BS, M, and MS treatments, PAH-RHDα GP amplicons were only detected in the heavy fractions from the [^{13}C]BaP-amended M and MS microcosms with the primer pair of 641f and 933r (Fig. 2), although both PAH-RHDα GP and PAH-RHDα GN primers were used to amplify PAH-RHDα genes in all treatments. In both treatments, the PAH-RHDα gene (PAH-RHDα-M) sequences shared 99% similarity with those of an uncultured strain (GenBank accession no. KF656719.1) and also high sequence similarity with affiliation to the genus *Mycobacterium*, which was capable of degrading BaP (15, 36). Recently, the microbial metabolism of low-molecular-weight (LMW) PAHs with no more than three rings has been studied extensively, including their metabolic pathways and enzymatic and genetic regulation (7). However, little is known about the metabolic pathways and genes related to BaP degradation and other HMW PAHs (37). Therefore, not all the functional genes derived from the active BaP-degrading bacteria could be detected by the primer sets used in this study.

PAH-RHDα-M genes in M and MS treatments were quantified against each density-resolved fraction (Fig. 3). A marked enrichment of PAH-RHDα-M genes in the heavy fractions (BD > 1.7200 g/ml) was observed in the [^{13}C]BaP-amended soils in MS treatment, indicating that the BD value of PAH-RHDα-M increased with [^{13}C]BaP degradation efficiency. In [^{12}C]BaP control, the majority of the PAH-RHDα-M genes were found in fractions with a BD of <1.7200 g/ml (Fig. 3A). For M treatment, no significant difference was observed between the ^{13}C-BT and ^{12}C-BT samples due to the limited changes in the PAH-RHDα-M genes and BD value (Fig. 3B). Hence, the detected PAH-RHDα-M genes were associated with BaP degradation in MS but not in M treatment, attributable to the salicylate addition, which significantly promoted the expression of PAH-RHDα-M genes, stimu-

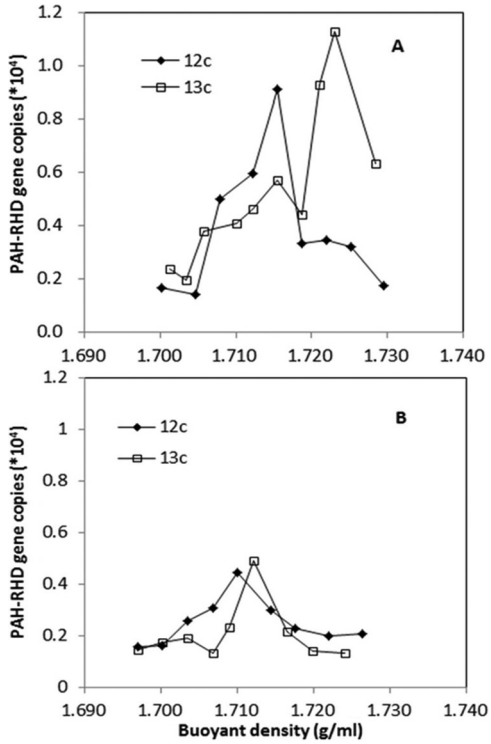

FIG 3 PAH-RHDα-M gene copies in ultracentrifugation fractions from [^{13}C]BaP- and [^{12}C]BaP-amended microcosms determined by qPCR. Panels A and B represent the microcosms from Mt. Maoer soil with and without salicylate addition. Symbols: □, [^{13}C]BaP (~52% BaP degraded); ■, [^{12}C]BaP (~42% BaP degraded).

lated PAH-RHDα-M-bearing bacteria, and improved BaP biodegradation.

DISCUSSION

Microorganisms responsible for the BaP degradation. DNA-SIP has been widely applied to the identification of pollutant degraders in numerous environmental media and with an ever-expanding pool of compounds (22, 27, 38). In the present study, the coupling of DNA-SIP and TRFLP techniques revealed the bacteria correlated with BaP metabolism in soils from Mt. Maoer and Mt. Baicaowa. Bacteria represented by 196-bp TRF were classified as members of the genus *Burkholderia* and were involved in BaP degradation in both B and BS treatments. *Burkholderia*-related bacteria have been linked with PAHs (39) and biphenyl (40) biodegradation in soil. As the dominant genus with key roles in the degradation of oil components (41), *Burkholderia* was found to be capable of degrading anthracene, phenanthrene, chrysene, and pyrene (7). Juhasz et al. found that a *Burkholderia cepacia* strain isolated from soil near a manufacturing gas plant could degrade BaP with pyrene as the carbon source, although only 1.4 to 6.2% BaP was removed after 56 days (42). A *Delftia* strain was isolated from the microbial consortium of a crude oil-contaminated soil and removed 56.6% BaP in PAH-contaminated soil after 14 days (43). To our knowledge, prior to this study, BaP degradation by *Burkholderia*-related microorganisms using DNA-SIP had not been documented.

In M treatment, microorganisms represented by the 450-bp TRF were correlated with BaP degradation and assigned to the genus *Terrimonas*. Sequence analysis suggested their close relationship to the *F. ginsengiterrae* strain Gsoil 492 (see Fig. S4 in the supplemental material). This strain was first isolated by Yoon and Im from soil used for ginseng planting, and it has the ability to grow with 3-hydroxybenzoic or 4-hydroxybenzoic acid as the sole carbon source (44). Strains of the genus *Sphingomonas* from the family *Sphingomonadaceae*, order *Sphingomonadales*, were able to degrade BaP with different cometabolic substances, and aqueous BaP at 1.2 mg/liter was completely removed within 20 h when *S. yanoikuyae* JAR02 grew on salicylate (8). Ye et al. also showed that 5% BaP was removed by *Sphingomonas paucimobilis* with fluoranthene as the cometabolic source of carbon and energy after 168 h when the initial concentration of BaP was 10 mg/liter (45). Until now, some strains affiliated with *Chitinophagaceae* were found in various environments and possessed the functions of metabolizing complex organic compounds. Though the crucial roles of these strains in carbon circulation were reported (46), little was known about their PAH-degrading capabilities. The present study showed that the genus *Terrimonas* correlated with BaP degradation, which expands our knowledge of this genus.

The bacteria involved in BaP degradation in the MS microcosm amended with BaP and salicylate were affiliated most closely with the family *Oxalobacteraceae* (phylum *Proteobacteria*, class *Betaproteobacteria*, order *Burkholderiales*; 216 bp). To date, many *Pseudomonas* strains in *Gammaproteobacteria* have been shown to possess the capability of degrading aromatic hydrocarbons such as pyrene, phenanthrene, naphthalene, toluene, and phenol in crude oil-contaminated soil (47). *Burkholderiales*-related bacteria in *Betaproteobacteria* were also related to PAH removal, and the family *Oxalobacteraceae* was widely found in PCB- and PAH-contaminated soils (40, 48). Huang et al. reported that a cultivated bacterial strain from the order *Burkholderiales* could degrade PAHs (41). However, no previous studies using SIP have demonstrated the BaP degradation capacity of *Burkholderiales*-related bacteria, and our results for Mt. Baicaowa soils suggest such possibilities.

The coupling of TRFLP with SIP enabled us to compare the TRFLP profiles over a range of BDs for both ^{13}C-labeled and unlabeled samples at different time intervals to avoid false-positive results. For example, in the M treatment, although three clones with predicted 237-, 372-, and 215-bp HaeIII cut sites were dominant in the 16S rRNA clone library, and the corresponding TRFs constituted a high proportion in the ^{13}C heavy fractions from [^{13}C]BaP-amended treatment, no significant difference was observed in these TRFs between the [^{13}C]BaP and [^{12}C]BaP treatments, suggesting their limited roles in *in situ* BaP degradation in our study.

The conflict between Gram-positive PAH-RHDα genes and detected Gram-negative BaP degraders is a puzzle. Such evolutionary distant has been explained previously as horizontal gene transfers of PAH-RHDα genes and other genes between Gram-positive and Gram-negative bacteria (49–52). For instance, the classical *nah*-like genes were shared among Gram-negative bacteria (49). *aphA-3*, an antibiotic resistance gene in *Campylobacter* encoding 3′-aminoglycoside phosphotransferases modifying the structure of kanamycin, was transferred between Gram-positive and Gram-negative bacteria (53). In our study, SIP results could not directly relate the Gram-positive PAH-RHDα genes to the functional Gram-negative host and therefore were not able to prove horizontal gene transfer. Further work is suggested for the single-cell isolation and genome amplification of individual BaP

degraders (54) and deeper investigation on the PAH-RHDα genes within the targeting functional species.

Effects of salicylate on BaP degradation and community structure. The addition of salicylate significantly changed the functional microbial community structure in the heavy fractions derived from the Mt. Baicaowa soils, but not the BaP degradation. The dominant species shifted from *Rhodanobacter*-related bacteria in the B microcosm to *Burkholderiales*-related bacteria in BS treatment, although *Acidobacteria*-related microorganisms existed in both treatments. The bacteria capable of degrading BaP (*Burkholderiales*) in B and BS treatments were detected as identical using DNA-SIP (see Table S1 in the supplemental material). Nevertheless, the similar BaP removal efficiency between the B and BS treatments hinted that BaP degradation was not stimulated by the functional microbial structure change and increasing *Burkholderiales*-related bacteria, consistent with a previous study by Powell (38). Since small pH variation might significantly affect the biodegradation of xenobiotics and other organic compounds in oligotrophic environments (55), the possible reason was the decreased PAH degradation activity of dominant *Burkholderiales*-related bacteria under low-pH conditions (56), like the pH of 6.0 in Mt. Baicaowa soils.

However, the TRFLP in M and MS treatments suggested that the addition of salicylate changed both functional microbial community structure in heavy fractions and BaP degradation rate (see Table S1 in the supplemental material). The dominant species correlated with BaP degradation shifted from *Terrimonas* to *Oxalobacteraceae* after the salicylate addition. The functional PAH-RHD genes might change (Fig. 3), and salicylate also accelerated the BaP degradation in Mt. Maoer microcosms (Table 1). Previous studies showed a significant increase in the rate of naphthalene mineralization in soil after enrichment with salicylate spiking (38). The presence of phenanthrene and salicylate also greatly enhanced the initial removal rates of benz[*a*]anthracene, chrysene, and benzo[*a*]pyrene by *P. saccharophila* P15 (16). The addition of salicylate to PAH-contaminated soils was shown to increase the quantity of naphthalene-degrading bacteria (57, 58) and stimulate the degradation of benzo[*a*]anthracene, chrysene (16), fluoranthene (16, 17), and BaP (8, 16). Salicylate was also reported to sustain populations of biological control bacteria with naphthalene-degrading genes in agricultural systems (59), and various salicylate additives (spiked or slow/continuous addition) have been used to select different microbial communities (38).

The effects of salicylate on PAH removal and functional microbial community structure depend on the soil properties and the bacterial profiles in the soils. Although salicylate is the central metabolite of many PAH degradation processes, it is not associated with some pathways, and its stimulating effect, therefore, might not be suitable for all cases of PAH degradation. For example, the addition of salicylate had no effect on phenanthrene or pyrene removal in PAH-contaminated soils (60). After enrichment with salicylate, the initial naphthalene mineralization rate, rather than those of phenanthrene and BaP, was enhanced by the microbial community in a bioreactor for a PAH-contaminated soil treatment (38). In uncontaminated soils, salicylate only improved pyrene removal and did not affect BaP (60), which may explain why salicylate stimulated BaP removal in Mt. Maoer soils but not Mt. Baicaowa soils.

In summary, three phylotypes in two different forest soils were linked with BaP degradation using the culture-independent SIP technique. The addition of salicylate affected the bacteria correlated with BaP metabolism and the BaP degradation efficiency differently in the two forest soils. In addition, a new PAH-RHDα gene involved in BaP metabolism was detected in the salicylate-amended soils from Mt. Maoer. Our results provide a deeper understanding of the contribution of SIP to identifying the functions of uncultured microorganisms, expand our knowledge on bacteria possessing the ability of BaP mineralization, and reveal specific effects of salicylate on the BaP biodegradation process.

ACKNOWLEDGMENTS

This study was supported by the Joint Funds of the National Natural Science Foundation of China and the Natural Science Foundation of Guangdong Province, China (no. U1133004), the National Natural Science Foundation of China (no. 41173082 and 41322008), and the Scientific and Technological Planning Project of Guangzhou, China (no. 201510010038).

REFERENCES

1. **Baek SO, Field RA, Goldstone ME, Kirk PW, Lester JN, Perry R.** 1991. A Review of atmospheric polycyclic aromatic-hydrocarbons—sources, fate and behavior. Water Air Soil Pollut **60:**279–300. http://dx.doi.org/10.1007/BF00282628.
2. **Zhang YX, Tao S.** 2009. Global atmospheric emission inventory of polycyclic aromatic hydrocarbons (PAHs) for 2004. Atmos Environ **43:**812–819. http://dx.doi.org/10.1016/j.atmosenv.2008.10.050.
3. **Keith LH, Telliard WA.** 1979. Priority pollutants I—a perspective view. Environ Sci Technol **13:**416–423. http://dx.doi.org/10.1021/es60152a601.
4. **Rodríguez-Fragoso L, Melendez K, Hudson LG, Lauer FT, Burchiel SW.** 2009. EGF-receptor phosphorylation and downstream signaling are activated by benzo[a]pyrene 3,6-quinone and benzo[a]pyrene 1,6-quinone in human mammary epithelial cells. Toxicol Appl Pharmacol **235:**321–328. http://dx.doi.org/10.1016/j.taap.2008.12.022.
5. **Wills LP, Zhu SQ, Willett KL, Di Giulio RT.** 2009. Effect of CYP1A inhibition on the biotransformation of benzo[a]pyrene in two populations of Fundulus heteroclitus with different exposure histories. Aquat Toxicol **92:**195–201. http://dx.doi.org/10.1016/j.aquatox.2009.01.009.
6. **IARC Working Group on the Evaluation of Carcinogenic Risks to Humans.** 2010. Household use of solid fuels and high-temperature frying. IARC Monogr Eval Carcinog Risks Hum **95:**9–38.
7. **Juhasz AL, Naidu R.** 2000. Bioremediation of high molecular weight polycyclic aromatic hydrocarbons: a review of the microbial degradation of benzo[a]pyrene. Int Biodeterior Biodegradation **45:**57–88. http://dx.doi.org/10.1016/S0964-8305(00)00052-4.
8. **Rentz JA, Alvarez PJJ, Schnoor JL.** 2008. Benzo[a]pyrene degradation by Sphingomonas yanoikuyae JAR02. Environ Pollut **151:**669–677. http://dx.doi.org/10.1016/j.envpol.2007.02.018.
9. **Peng H, Yin H, Deng J, Ye JS, Chen SN, He BY, Zhang N.** 2012. Biodegradation of benzo[a]pyrene by Arthrobacter oxydans B4. Pedosphere **22:**554–561. http://dx.doi.org/10.1016/S1002-0160(12)60040-X.
10. **Mishra S, Singh SN.** 2014. Biodegradation of benzo(a)pyrene mediated by catabolic enzymes of bacteria. Int J Environ Sci Technol (Tehran) **11:**1571–1580. http://dx.doi.org/10.1007/s13762-013-0300-6.
11. **Jurelevicius D, Alvarez VM, Peixoto R, Rosado AS, Seldin L.** 2012. Bacterial polycyclic aromatic hydrocarbon ring-hydroxylating dioxygenases (PAH-RHD) encoding genes in different soils from King George Bay, Antarctic Peninsula. Appl Soil Ecol **55:**1–9. http://dx.doi.org/10.1016/j.apsoil.2011.12.008.
12. **Cébron A, Norini MP, Beguiristain T, Leyval C.** 2008. Real-time PCR quantification of PAH-ring hydroxylating dioxygenase (PAH-RHD alpha) genes from Gram positive and Gram negative bacteria in soil and sediment samples. J Microbiol Methods **73:**148–159. http://dx.doi.org/10.1016/j.mimet.2008.01.009.
13. **Lily MK, Bahuguna A, Dangwal K, Garg V.** 2009. Degradation of benzo [a] pyrene by a novel strain Bacillus subtilis Bmt4i (Mtcc 9447). Braz J Microbiol **40:**884–892. http://dx.doi.org/10.1590/S1517-83822009000400020.
14. **Kanaly RA, Harayama S.** 2000. Biodegradation of high-molecular-weight polycyclic aromatic hydrocarbons by bacteria. J Bacteriol **182:**2059–2067. http://dx.doi.org/10.1128/JB.182.8.2059-2067.2000.

15. **Kanaly RA, Harayama S.** 2010. Advances in the field of high-molecular-weight polycyclic aromatic hydrocarbon biodegradation by bacteria. Microb Biotechnol **3:**136–164. http://dx.doi.org/10.1111/j.1751-7915.2009.00130.x.
16. **Chen SH, Aitken MD.** 1999. Salicylate stimulates the degradation of high molecular weight polycyclic aromatic hydrocarbons by Pseudomonas saccharophila P15. Environ Sci Technol **33:**435–439. http://dx.doi.org/10.1021/es9805730.
17. **Alemayehu D, Gordon LM, O'Mahony MM, O'Leary ND, Dobson ADW.** 2004. Cloning and functional analysis gene involved in indigo production by gene disruption of a novel and fluoranthene metabolism in Pseudomonas alcaligenes PA-10. FEMS Microbiol Lett **239:**285–293. http://dx.doi.org/10.1016/j.femsle.2004.08.046.
18. **Bode HB, Muller R.** 2005. The impact of bacterial genomics on natural product research. Angew Chem Int Ed **44:**6828–6846. http://dx.doi.org/10.1002/anie.200501080.
19. **Galvão TC, Mohn WW, de Lorenzo V.** 2005. Exploring the microbial biodegradation and biotransformation gene pool. Trends Biotechnol **23:**497–506. http://dx.doi.org/10.1016/j.tibtech.2005.08.002.
20. **Lorenz P, Eck J.** 2005. Metagenomics and industrial applications. Nat Rev Microbiol **3:**510–516. http://dx.doi.org/10.1038/nrmicro1161.
21. **Oren A.** 2004. Prokaryote diversity and taxonomy: current status and future challenges. Philos Trans R Soc Lond B Biol Sci. **359:**623–638. http://dx.doi.org/10.1098/rstb.2003.1458.
22. **Radajewski S, Ineson P, Parekh NR, Murrell JC.** 2000. Stable-isotope probing as a tool in microbial ecology. Nature **403:**646–649. http://dx.doi.org/10.1038/35001054.
23. **Singleton DR, Sangaiah R, Gold A, Ball LM, Aitken MD.** 2006. Identification and quantification of uncultivated Proteobacteria associated with pyrene degradation in a bioreactor treating PAH-contaminated soil. Environ Microbiol **8:**1736–1745. http://dx.doi.org/10.1111/j.1462-2920.2006.01112.x.
24. **Luo CL, Xie SG, Sun WM, Li XD, Cupples AM.** 2009. Identification of a novel toluene-degrading bacterium from the candidate phylum TM7, as determined by DNA stable isotope probing. Appl Environ Microbiol **75:**4644–4647. http://dx.doi.org/10.1128/AEM.00283-09.
25. **Gutierrez T, Singleton DR, Aitken MD, Semple KT.** 2011. Stable isotope probing of an algal bloom to identify uncultivated members of the Rhodobacteraceae associated with low-molecular-weight polycyclic aromatic hydrocarbon degradation. Appl Environ Microbiol **77:**7856–7860. http://dx.doi.org/10.1128/AEM.06200-11.
26. **Singleton DR, Powell SN, Sangaiah R, Gold A, Ball LM, Aitken MD.** 2005. Stable-isotope probing of bacteria capable of degrading salicylate, naphthalene, or phenanthrene in a bioreactor treating contaminated soil. Appl Environ Microbiol **71:**1202–1209. http://dx.doi.org/10.1128/AEM.71.3.1202-1209.2005.
27. **Zhang SY, Wang QF, Xie SG.** 2012. Stable isotope probing identifies anthracene degraders under methanogenic conditions. Biodegradation **23:**221–230. http://dx.doi.org/10.1007/s10532-011-9501-1.
28. **Peng JJ, Zhang Y, Su JQ, Qiu QF, Jia ZJ, Zhu YG.** 2013. Bacterial communities predominant in the degradation of C-13(4)-4,5,9,10-pyrene during composting. Bioresour Technol **143:**608–614. http://dx.doi.org/10.1016/j.biortech.2013.06.039.
29. **Jones MD, Crandell DW, Singleton DR, Aitken MD.** 2011. Stable-isotope probing of the polycyclic aromatic hydrocarbon-degrading bacterial guild in a contaminated soil. Environ Microbiol **13:**2623–2632. http://dx.doi.org/10.1111/j.1462-2920.2011.02501.x.
30. **Sul WJ, Park J, Quensen JF, Rodrigues JLM, Seliger L, Tsoi TV, Zylstra GJ, Tiedje JM.** 2009. DNA-stable isotope probing integrated with metagenomics for retrieval of biphenyl dioxygenase genes from polychlorinated biphenyl-contaminated river sediment. Appl Environ Microbiol **75:**5501–5506. http://dx.doi.org/10.1128/AEM.00121-09.
31. **Uhlik O, Wald J, Strejcek M, Musilova L, Ridl J, Hroudova M, Vlcek C, Cardenas E, Mackova M, Macek T.** 2012. Identification of bacteria utilizing biphenyl, benzoate, and naphthalene in long-term contaminated soil. PLoS One **7**(7):e40653. http://dx.doi.org/10.1371/journal.pone.0040653.
32. **Mu DY, Scow KM.** 1994. Effect of trichloroethylene (Tce) and toluene concentrations on Tce and toluene biodegradation and the population density of Tce and toluene degraders in soil. Appl Environ Microbiol **60:**2661–2665.
33. **Sun WM, Xie SG, Luo CL, Cupples AM.** 2010. Direct link between toluene degradation in contaminated-site microcosms and a Polaromonas strain. Appl Environ Microbiol **76:**956–959. http://dx.doi.org/10.1128/AEM.01364-09.
34. **Cupples AM, Sims GK.** 2007. Identification of in situ 2,4-dichlorophenoxyacetic acid-degrading soil microorganisms using DNA-stable isotope probing. Soil Biol Biochem **39:**232–238. http://dx.doi.org/10.1016/j.soilbio.2006.07.011.
35. **Sun WM, Cupples AM.** 2012. Diversity of five anaerobic toluene-degrading microbial communities investigated using stable isotope probing. Appl Environ Microbiol **78:**972–980. http://dx.doi.org/10.1128/AEM.06770-11.
36. **Warshawsky D, Ladow K, Schneider J.** 2007. Enhanced degradation of benzo[a]pyrene by Mycobacterium sp in conjunction with green alga. Chemosphere **69:**500–506. http://dx.doi.org/10.1016/j.chemosphere.2007.03.031.
37. **Moody JD, Freeman JP, Fu PP, Cerniglia CE.** 2004. Degradation of benzo[a]pyrene by Mycobacterium vanbaalenii PYR-1. Appl Environ Microbiol **70:**340–345. http://dx.doi.org/10.1128/AEM.70.1.340-345.2004.
38. **Powell SN, Singleton DR, Aitken MD.** 2008. Effects of enrichment with salicylate on bacterial selection and PAH mineralization in a microbial community from a bioreactor treating contaminated soil. Environ Sci Technol **42:**4099–4105. http://dx.doi.org/10.1021/es703007n.
39. **Ang EL, Zhao HM, Obbard JP.** 2005. Recent advances in the bioremediation of persistent organic pollutants via biomolecular engineering. Enzyme Microb Technol **37:**487–496. http://dx.doi.org/10.1016/j.enzmictec.2004.07.024.
40. **de Carcer DA, Martin M, Karlson U, Rivilla R.** 2007. Changes in bacterial populations and in biphenyl dioxygenase gene diversity in a polychlorinated biphenyl-polluted soil after introduction of willow trees for rhizoremediation. Appl Environ Microbiol **73:**6224–6232. http://dx.doi.org/10.1128/AEM.01254-07.
41. **Huang X, Luo Y, Hu Z, Tian Y.** 2006. Recent advance in the study of persistent organic pollutants bioremediation. Acta Sci Circum **26:**353–361.
42. **Juhasz AL, Britz ML, Stanley GA.** 1997. Degradation of benzo[a]pyrene, dibenz[a,h]anthracene and coronene by Burkholderia cepacia. Water Sci Technol **36:**45–51.
43. **Zafra G, Absalon AE, Cuevas MD, Cortes-Espinosa DV.** 2014. Isolation and selection of a highly tolerant microbial consortium with potential for PAH biodegradation from heavy crude oil-contaminated soils. Water Air Soil Pollut **225:**1826. http://dx.doi.org/10.1007/s11270-013-1826-4.
44. **Yoon MH, Im WT.** 2007. Flavisolibacter ginsengiterrae gen. nov., sp nov and Flavisolibacter ginsengisoli sp nov., isolated from ginseng cultivating soil. Int J Syst Evol Microbiol **57:**1834–1839. http://dx.doi.org/10.1099/ijs.0.65011-0.
45. **Ye DY, Siddiqi MA, Maccubbin AE, Kumar S, Sikka HC.** 1996. Degradation of polynuclear aromatic hydrocarbons by Sphingomonas paucimobilis. Environ Sci Technol **30:**136–142. http://dx.doi.org/10.1021/es9501878.
46. **Everard A, Lazarevic V, Derrien M, Girard M, Muccioli GG, Neyrinck AM, Possemiers S, Van Holle A, Francois P, de Vos WM, Delzenne NM, Schrenzel J, Cani PD.** 2011. Responses of gut microbiota and glucose and lipid metabolism to prebiotics in genetic obese and diet-induced leptin-resistant mice. Diabetes **60:**3307–3307. http://dx.doi.org/10.2337/db11-er12c.
47. **Chang H, Nie M, Ge B, Liu C, Yang Q, Zhou L, Fan X, Sun C.** 2013. Effects of rhamnolipid on oil degradation by Pseudomonas aeruginosa strain NY3. Chin J Environ Eng **7:**771–776.
48. **Tejeda-Agredano MC, Gallego S, Vila J, Grifoll M, Ortega-Calvo JJ, Cantos M.** 2013. Influence of the sunflower rhizosphere on the biodegradation of PAHs in soil. Soil Biol Biochem **57:**830–840. http://dx.doi.org/10.1016/j.soilbio.2012.08.008.
49. **Habe H, Omori T.** 2003. Genetics of polycyclic aromatic hydrocarbon metabolism in diverse aerobic bacteria. Biosci Biotechnol Biochem **67:**225–243. http://dx.doi.org/10.1271/bbb.67.225.
50. **Herrick JB, Stuart-Keil KG, Ghiorse WC, Madsen EL.** 1997. Natural horizontal transfer of a naphthalene dioxygenase gene between bacteria native to a coal tar-contaminated field site. Appl Environ Microbiol **63:**2330–2337.
51. **Wilson MS, Herrick JB, Jeon CO, Hinman DE, Madsen EL.** 2003. Horizontal transfer of phnAc dioxygenase genes within one of two phenotypically and genotypically distinctive naphthalene-degrading guilds from adjacent soil environments. Appl Environ Microbiol **69:**2172–2181. http://dx.doi.org/10.1128/AEM.69.4.2172-2181.2003.

52. **Yagi JM, Sims D, Brettin T, Bruce D, Madsen EL.** 2009. The genome of Polaromonas naphthalenivorans strain CJ2, isolated from coal tar-contaminated sediment, reveals physiological and metabolic versatility and evolution through extensive horizontal gene transfer. Environ Microbiol **11:**2253–2270. http://dx.doi.org/10.1111/j.1462-2920.2009.01947.x.
53. **Trieu-Cuot P, Gerbaud G, Lambert T, Courvalin P.** 1985. In vivo transfer of genetic information between gram-positive and gram-negative bacteria. EMBO J **4:**3583–3587.
54. **Zhang DY, Berry JP, Zhu D, Wang Y, Chen Y, Jiang B, Huang S, Langford H, Li GH, Davison PA, Xu J, Aries E, Huang WE.** 2015. Magnetic nanoparticle-mediated isolation of functional bacteria in a complex microbial community. ISME J **9:**603–614. http://dx.doi.org/10.1038/ismej.2014.161.
55. **Kästner M, Breuer-Jammali M, Mahro B.** 1998. Impact of inoculation protocols, salinity, and pH on the degradation of polycyclic aromatic hydrocarbons (PAHs) and survival of PAH-degrading bacteria introduced into soil. Appl Environ Microbiol **64:**359–362.
56. **Wong JWC, Lai KM, Wan CK, Ma KK, Fang M.** 2002. Isolation and optimization of PAH-degradative bacteria from contaminated soil for PAHs bioremediation. Water Air Soil Pollut **139:**1–13. http://dx.doi.org/10.1023/A:1015883924901.
57. **Ogunseitan OA, Delgado IL, Tsai YL, Olson BH.** 1991. Effect of 2-hydroxybenzoate on the maintenance of naphthalene-degrading pseudomonads in seeded and unseeded soil. Appl Environ Microbiol **57:**2873–2879.
58. **Ogunseitan OA, Olson BH.** 1993. Effect of 2-hydroxybenzoate on the rate of naphthalene mineralization in soil. Appl Microbiol Biot **38:**799–807. http://dx.doi.org/10.1007/BF00167148.
59. **Ji PS, Wilson M.** 2003. Enhancement of population size of a biological control agent and efficacy in control of bacterial speck of tomato through salicylate and ammonium sulfate amendments. Appl Environ Microbiol **69:**1290–1294. http://dx.doi.org/10.1128/AEM.69.2.1290-1294.2003.
60. **Carmichael LM, Pfaender FK.** 1997. The effect of inorganic and organic supplements on the microbial degradation of phenanthrene and pyrene in soils. Biodegradation **8:**1–13. http://dx.doi.org/10.1023/A:1008258720649.